

# Assessment of P-Glycoprotein in Patients with Malignant Bone and Soft-Tissue Tumors Using Technetium-99m-MIBI Scintigraphy

Junichi Taki, Hisashi Sumiya, Naohiro Asada, Yoshimichi Ueda, Hiroyuki Tsuchiya and Norihisa Tonami  
Departments of Nuclear Medicine and Orthopedics, Kanazawa University School of Medicine, Kanazawa;  
and Department of Pathology, Kanazawa Medical University, Uchinada, Japan

Overexpression of P-glycoprotein (Pgp) has been detected in many malignant tumors including bone and soft-tissue tumors. Technetium-99m-MIBI has proved to be a transport substrate for Pgp. The purpose of our study was to explore  $^{99m}\text{Tc}$ -MIBI as a functional imaging agent reflecting Pgp expression in malignant bone and soft-tissue tumors. **Methods:** Technetium-99m-MIBI scintigraphy was performed in 30 patients with malignant bone and soft-tissue tumors. Radionuclide angiography with  $^{99m}\text{Tc}$ -MIBI was done and, at 15 min and 3 hr postinjection of the radiopharmaceutical, imaging was performed. The  $^{99m}\text{Tc}$ -MIBI uptake ratio was calculated by dividing the lesion count by the background count. The washout rate (WR) for  $^{99m}\text{Tc}$ -MIBI was calculated by the following formula:  $\text{WR} = 100 \times [(\text{Te}-\text{Be})-(\text{Td}-\text{Bd})]/(\text{Te}-\text{Be})$  (%), where Te and Td = decay-corrected count density of the tumor in the 15-min and 3-hr images, respectively. Be and Bd = decay-corrected count density of the background in the 15-min and 3-hr images, respectively. The lesions were resected by open biopsy to obtain a histopathological diagnosis, and immunohistochemical staining was performed to detect Pgp. **Results:** Twenty-four of 30 patients showed significant uptake at the 15-min image. In these 24 patients, the lesions with a high Pgp expression showed a similar  $^{99m}\text{Tc}$ -MIBI perfusion index ( $3.00 \pm 1.04$ ) and uptake ratio ( $2.05 \pm 0.58$ ) at the 15-min image to those of lesions without a high Pgp expression ( $2.65 \pm 0.85$  and  $2.28 \pm 0.64$ , respectively). On delayed images, the  $^{99m}\text{Tc}$ -MIBI uptake ratio was lower in patients with a high Pgp expression than in patients without a high Pgp expression ( $1.37 \pm 0.41$  versus  $1.87 \pm 0.39$ ,  $p < 0.01$ ). The washout ratio of  $^{99m}\text{Tc}$ -MIBI was higher in patients with a high Pgp expression than in patients without a high Pgp expression ( $66\% \pm 25\%$  versus  $29\% \pm 18\%$ ,  $p < 0.001$ ). None of the 6 patients without  $^{99m}\text{Tc}$ -MIBI uptake at the 15-min imaging showed  $^{201}\text{Tl}$  uptake, and only 2 had a high Pgp expression. **Conclusion:** In malignant bone and soft-tissue tumors, perfusion and initial  $^{99m}\text{Tc}$ -MIBI uptake were not related to the Pgp expression; however, washout of  $^{99m}\text{Tc}$ -MIBI from the tumor was related to Pgp expression. Technetium-99m-MIBI scintigraphy with washout analysis may be a useful method for the evaluation of Pgp overexpression and its function.

**Key Words:** technetium-99m-MIBI; P-glycoprotein; multidrug resistance; bone tumor; soft-tissue tumor

**J Nucl Med 1998; 39:1179-1184**

Recently,  $^{99m}\text{Tc}$ -hexakis-2-methoxyisobutylisonitrile (MIBI), used as a myocardial perfusion imaging agent, has demonstrated promise as an imaging agent for various tumors including bone and soft-tissue tumors (1-7). In bone and soft-tissue malignant tumors, preoperative chemotherapy has been a standard therapeutic method (8,9). However, drug resistance is a major problem in chemotherapy. One of the important mechanisms responsible for this resistance is the overexpression of the

multidrug resistance gene (MDR1) (10). This gene encodes a 170-KDa P-glycoprotein (Pgp), an adenosine triphosphate-dependent transmembrane pump, which extrudes a structurally and functionally diverse group of chemotherapeutic compounds including anthracyclines, vinca alkaloids, actinomycin D and epipodophyllotoxins (11). MDR1 expression is not rare in bone and soft-tissue sarcomas. Noonan et al. (12) reported that 26 of 92 bone and soft-tissue sarcomas showed high levels of MDR1 expression, 44 demonstrated low levels and 20 showed no evidence of MDR1 expression. It was disclosed recently that  $^{99m}\text{Tc}$ -MIBI, a lipophilic cation used for myocardial perfusion imaging, is also a substrate for Pgp based on findings that  $^{99m}\text{Tc}$ -MIBI showed a lower accumulation in Pgp-enriched hamster and rat cell lines compared to their respective parental drug-sensitive cell lines (13,14). A similar result also was obtained with human tumor cells (13,15).

The aim of our study was to explore the potential of  $^{99m}\text{Tc}$ -MIBI as a functional imaging agent reflecting Pgp expression in malignant bone and soft-tissue tumors in a clinical setting. For this purpose, the  $^{99m}\text{Tc}$ -MIBI uptake pattern of the tumors and the degree of Pgp expression of the biopsy specimens were compared.

## MATERIALS AND METHODS

### Patients

Our study comprised 30 patients with various malignant bone and soft-tissue tumors proven pathologically by specimens obtained from biopsy and/or surgery. There were 30 patients (12 women, 18 men; age range, 8-81 yr; mean age, 46 yr  $\pm$  22 yr). All 30 patients had malignant tumors: (a) 4 osteosarcomas; (b) 4 chondrosarcomas; (c) 6 malignant fibrous histiocytomas, 3 were a recurrence; (d) 2 liposarcomas, 1 was a recurrence; (e) 2 malignant schwannomas; (f) 1 parosteal osteosarcoma; (g) 1 epithelioid sarcoma; (h) 1 synovial cell sarcoma; (i) 1 extraskeletal myxoid chondrosarcoma; (j) 1 Ewing's sarcoma; (k) 1 non-Hodgkin's lymphoma; (l) 1 fibromyxoid sarcoma; and (m) 5 bone metastatic tumors (adenocarcinoma).

### Technetium-99m-MIBI and Thallium-201 Scintigraphy

Radionuclide angiography was performed postinjection of 600-740 MBq  $^{99m}\text{Tc}$ -MIBI with a gamma camera equipped with a low-energy, high-resolution parallel-hole collimator. Data were acquired every 2 sec for 2 min. Then, planar 2- or 3-min  $^{99m}\text{Tc}$ -MIBI images of the lesions and the anterior chest were obtained at 15 min and 3 hr after radionuclide administration.

When  $^{99m}\text{Tc}$ -MIBI uptake was not observed in early imaging, within 1 wk of the  $^{99m}\text{Tc}$ -MIBI study, planar 2- or 3-min  $^{201}\text{Tl}$  imaging was performed at 15 min after intravenous injection of 111 MBq of the radiopharmaceutical with a gamma camera equipped with a low-energy, high-resolution parallel-hole collimator.

Received Jun. 9, 1997; revision accepted Oct. 13, 1997.

For correspondence or reprints contact: Junichi Taki, MD, Department of Nuclear Medicine, Kanazawa University School of Medicine, 13-1 Takara-machi, Kanazawa, 9208640 Japan.

**TABLE 1**  
P-Glycoprotein Expression and Scintigraphic Findings with Technetium-99m-MIBI

| Patient no.   | Age (yr) /sex | Diagnosis                           | Site of lesion             | Tumor size (cm) | PgP score | Technetium-99m-MIBI |                 |              |          |
|---|---------------|-------------------------------------|----------------------------|-----------------|-----------|---------------------|-----------------|--------------|----------|
|   |               |                                     |                            |                 |           | Washout rate (%)    | Perfusion index | Uptake ratio |          |
|   |               |                                     |                            |                 |           |                     |                 | 15 min       | 3 hr     |
| <i>Patients without MIBI uptake on 15-min image</i> |               |                                     |                            |                 |           |                     |                 |              |          |
| 1   | 53/M          | Myxoid liposarcoma                  | Right thigh                | 9 × 5 × 4       | 0         | —                   | 1.05 (0)        | 1.13 (0)     | 1.10 (0) |
| 2   | 28/M          | Chondrosarcoma                      | Right pelvis               | 11 × 8 × 5      | 0         | —                   | 1.55 (1)        | 1.07 (0)     | 1.00 (0) |
| 3   | 46/F          | Liposarcoma*                        | Left retroperitoneal space | 2 × 2 × 1       | 0         | —                   | 1.01 (0)        | 0.96 (0)     | 0.90 (0) |
| 4   | 32/F          | Chondrosarcoma                      | Left femur                 | 6 × 4 × 4       | 0         | —                   | 1.01 (0)        | 0.86 (0)     | 0.80 (0) |
| 5   | 16/M          | Malignant schwannoma                | Cervical spine             | 3 × 2 × 2       | 2         | —                   | 1.08 (0)        | 1.03 (0)     | 1.00 (0) |
| 6   | 23/M          | Osteosarcoma                        | Sacrum                     | 10 × 5 × 4      | 2         | —                   | 0.98 (0)        | 1.02 (0)     | 0.97 (0) |
| <i>Patients with MIBI uptake on 15-min image</i>    |               |                                     |                            |                 |           |                     |                 |              |          |
| 7   | 35/F          | Synovial cell sarcoma               | Left plantar pedis         | 6 × 3 × 3       | 0         | 26                  | 3.17 (2)        | 2.48 (2)     | 2.32 (2) |
| 8   | 72/F          | Non-Hodgkin's lymphoma              | Left buttock               | 12 × 10 × 10    | 0         | 24                  | 2.29 (2)        | 2.43 (3)     | 1.99 (2) |
| 9   | 74/M          | Malignant fibrous histiocytoma*     | Right upper arm            | 4 × 3 × 3       | 0         | 3                   | 1.80 (1)        | 1.39 (1)     | 1.51 (1) |
| 10  | 44/M          | Extraskelatal myxoid chondrosarcoma | Left upper arm             | 10 × 7 × 6      | 0         | 55                  | 2.66 (3)        | 2.19 (3)     | 1.60 (1) |
| 11  | 23/F          | Malignant Schwannoma                | Right axilla               | 10 × 8 × 7      | 1         | 23                  | 1.33 (0)        | 2.56 (3)     | 2.27 (2) |
| 12  | 69/M          | Malignant fibrous histiocytoma†     | Right thigh                | 10 × 4 × 3      | 1         | 17                  | 1.94 (1)        | 1.53 (2)     | 1.48 (1) |
| 13  | 66/F          | Malignant fibrous histiocytoma      | Left buttock               | 17 × 15 × 14    | 1         | 27                  | 3.54 (2)        | 1.86 (2)     | 1.31 (1) |
| 14  | 67/M          | Metastatic adenocarcinoma           | Right pelvic bone          | 11 × 8 × 6      | 1         | 21                  | 3.55 (3)        | 2.62 (2)     | 2.28 (1) |
| 15  | 67/F          | Malignant fibrous histiocytoma      | Right femur                | 6 × 5 × 5       | 1         | 61                  | 3.56 (3)        | 3.48 (3)     | 2.03 (1) |
| 16  | 16/M          | Osteosarcoma                        | Right humerus              | 10 × 5 × 5      | 2         | 68                  | 2.81 (2)        | 1.62 (2)     | 1.04 (0) |
| 17  | 8/M           | Ewing's sarcoma                     | Right humerus              | 10 × 6 × 6      | 2         | 44                  | 2.19 (2)        | 2.50 (2)     | 1.96 (1) |
| 18  | 73/F          | Chondrosarcoma                      | Left femur                 | 20 × 10 × 8     | 2         | 19                  | 2.66 (3)        | 1.50 (1)     | 1.44 (1) |
| 19  | 64/M          | Malignant fibrous histiocytoma†     | Right pelvis               | 12 × 10 × 9     | 2         | 82                  | 2.52 (2)        | 2.11 (2)     | 1.11 (0) |
| 20  | 39/M          | Malignant fibrous histiocytoma      | Lumbar subcutaneum         | 3 × 2 × 2       | 2         | 79                  | 1.83 (1)        | 1.61 (2)     | 1.08 (0) |
| 21  | 34/F          | Parosteal osteosarcoma              | Right femur                | 5 × 3 × 2       | 2         | 37                  | 2.47 (2)        | 1.61 (2)     | 1.32 (1) |
| 22  | 58/M          | Epithelioid sarcoma                 | Right thigh                | 10 × 5 × 5      | 2         | 71                  | 4.36 (3)        | 2.30 (3)     | 1.30 (1) |
| 23  | 14/M          | Osteosarcoma                        | Right tibia                | 6 × 4 × 3       | 2         | 76                  | 3.00 (2)        | 2.32 (2)     | 1.19 (0) |
| 24  | 67/F          | Metastatic adenocarcinoma           | Sacrum                     | 4 × 3 × 3       | 2         | 55                  | 1.93 (1)        | 1.87 (1)     | 1.47 (0) |
| 25  | 81/M          | Chondrosarcoma                      | Right thumb                | 3 × 2 × 1       | 3         | 100                 | 2.39 (2)        | 1.47 (2)     | 1.04 (1) |
| 26  | 49/M          | Metastatic adenocarcinoma           | Left femur                 | 8 × 8 × 7       | 3         | 45                  | 4.48 (3)        | 2.56 (3)     | 1.71 (2) |
| 27  | 61/F          | Metastatic adenocarcinoma           | Left femur                 | 6 × 5 × 4       | 3         | 49                  | 3.93 (3)        | 3.60 (3)     | 2.50 (3) |
| 28  | 9/F           | Osteosarcoma                        | Left femur                 | 7 × 5 × 4       | 3         | 100                 | 4.34 (3)        | 1.86 (2)     | 1.10 (0) |
| 29  | 48/M          | Fibromyxoid sarcoma                 | Left calf                  | 15 × 8 × 6      | 3         | 100                 | 4.51 (3)        | 2.31 (3)     | 1.06 (0) |
| 30  | 48/M          | Metastatic adenocarcinoma           | Left femur                 | 12 × 4 × 4      | 3         | 58                  | 1.61 (2)        | 1.50 (2)     | 1.22 (1) |

\*Recurrence after operation.

†Recurrence after chemotherapy and operation.

Pgp = p-glycoprotein; numerals in parentheses = visual perfusion and uptake scores.

### Image Analysis

Both <sup>99m</sup>Tc-MIBI and <sup>201</sup>Tl images were evaluated visually and quantitatively. In visual analysis, two blinded observers evaluated the degree of radionuclide uptake using a five-grade scoring system: (a) 0 = background activity; (b) 1+ = slight increase in uptake; (c) 2+ = moderate uptake; (d) 3+ = strong uptake, but less than heart; (e) 4+ = strong uptake equal to or greater than heart. Radionuclide angiography with <sup>99m</sup>Tc-MIBI also was evaluated by two blinded observers and the degree of perfusion increase was classified into four grades: (a) 0 = no increase; (b) 1+ = mild increase; (c) 2+ = moderate increase; (d) 3+ = marked increase in arterial phase (7).

In quantitative analysis, on the 15-min image, a manual region of interest (ROI) was set on the lesion and a symmetrical ROI was set on the contralateral normal area as a background. When radionuclide activity around the lesion was different from that of the normal side, for example, due to decreased radionuclide uptake by disuse atrophy of the affected extremities, background ROI was set on the region adjacent to the tumors. The same ROIs were used for the analysis of the 3-hr image. The uptake ratio was calculated by dividing the count density of the lesion by that of the background

ROI. The washout rate (WR) of <sup>99m</sup>Tc-MIBI from the lesions was calculated by the following formula:

$$WR (\%) = \frac{100 \times [(Te - Be) - (Td - Bd)]}{(Te - Be)}, \quad \text{Eq. 1}$$

where Te = decay-corrected count density of the tumor in the 15-min image; Td = decay-corrected count density of the tumor in the 3-hr image; Be = decay-corrected count density of the background in the 15-min image; Bd = decay-corrected count density of the background in the 3-hr image. WR was corrected by dividing by the ratio of the actual time interval between the 15-min and the 3-hr imaging to 165 min.

The perfusion index was obtained by radionuclide angiography. Using the same ROI set to calculate the uptake ratio, the time-activity curve of each ROI was generated and the perfusion index was determined by dividing the peak count of the arterial phase of the lesion by that of the background ROI. When a peak count was not obtained, the time-activity curve always showed a shoulder point, which was the turning point between the rapid count increase due to the arterial phase and the steady state or gradual count increase due to <sup>99m</sup>Tc-MIBI accumulation to lesion and normal

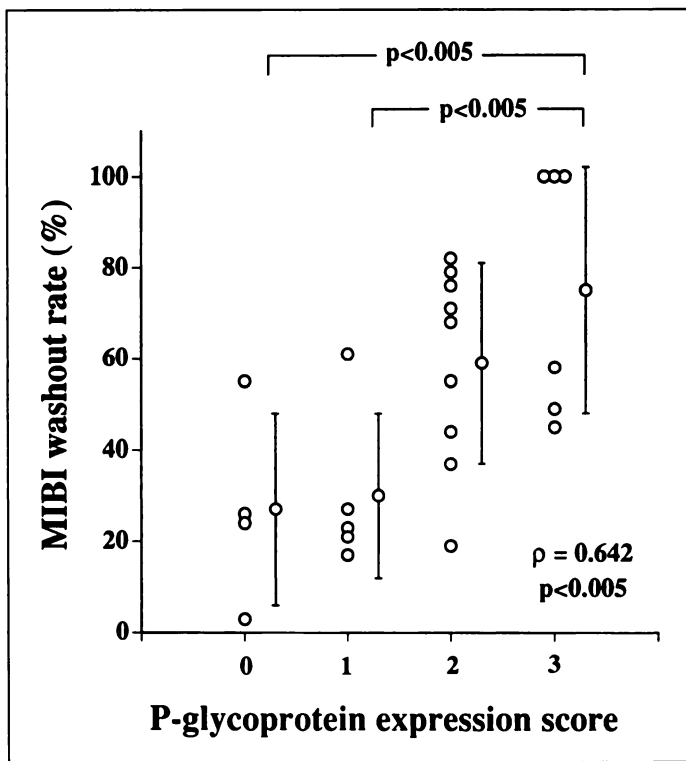


**FIGURE 1.** Technetium-99m-MIBI washout rate in each P-glycoprotein expression score. Significant differences in  $^{99m}\text{Tc}$ -MIBI washout were observed between patients with Pgp scores 0 and 3 ( $p < 0.005$ ) and 1 and 3 ( $p < 0.005$ ). Tumors with high P-glycoprotein expression demonstrated higher  $^{99m}\text{Tc}$ -MIBI washout from lesions. There was a positive correlation between  $^{99m}\text{Tc}$ -MIBI washout rate and Pgp expression ( $r = 0.642$ ,  $p < 0.005$ ).

tissue. The count of the turning point of the time-activity curve was used to calculate the perfusion index (7).

#### Detection of P-Glycoprotein Expression

The lesions were resected by open biopsy to obtain a histopathological diagnosis within 1 wk after  $^{99m}\text{Tc}$ -MIBI imaging. Immunohistochemical staining was performed according to the standard streptavidin-biotin method. The primary antibody applied for P-glycoprotein was NCL-pGLYp (1:20, Novocastra Laboratories Ltd., Newcastle, UK), a rabbit polyclonal antibody raised with synthetic peptide corresponding to an intracellular epitope in the carboxy terminal region of P-glycoprotein. We evaluated this antibody and JSB-1, a monoclonal antibody (Novocastra Laboratories Ltd., Newcastle, UK) (16,17). NCL-pGLYp showed the least variation in the results of immunostaining in different experiments and produced uniform results in tissue sections, especially in decalcified specimens, and demonstrated specific stain as had been observed with JSB-1. Sections of tissue were fixed in formaldehyde solution and embedded in paraffin, then they were cut out and mounted on silane-coated glass slides. The sections were deparaffinized with xylene for 30 min and washed in 100% ethanol twice. After inhibition of endogenous peroxidase with 30%  $\text{H}_2\text{O}_2$ /methanol and nonspecific binding of antibody by 10% normal goat serum, primary antibody was applied for 24 hr at 4°C. Tissue sections from a normal kidney were used because the reactivity of proximal tubules differs from that of glomeruli, so that results of Pgp immunostaining are positive in proximal tubules and negative in glomeruli (17–19). Color was developed with diaminobenzidine, and nuclear staining was done with Meyer's hematoxylin. The degree of Pgp expression was scored from 0–3 based on the distribution of positivity of immunostaining of the plasma membrane and the Golgi region (17) as follows: (a) Score 0 when no stain was observed; (b) Score 1 when less than 10% of the cells

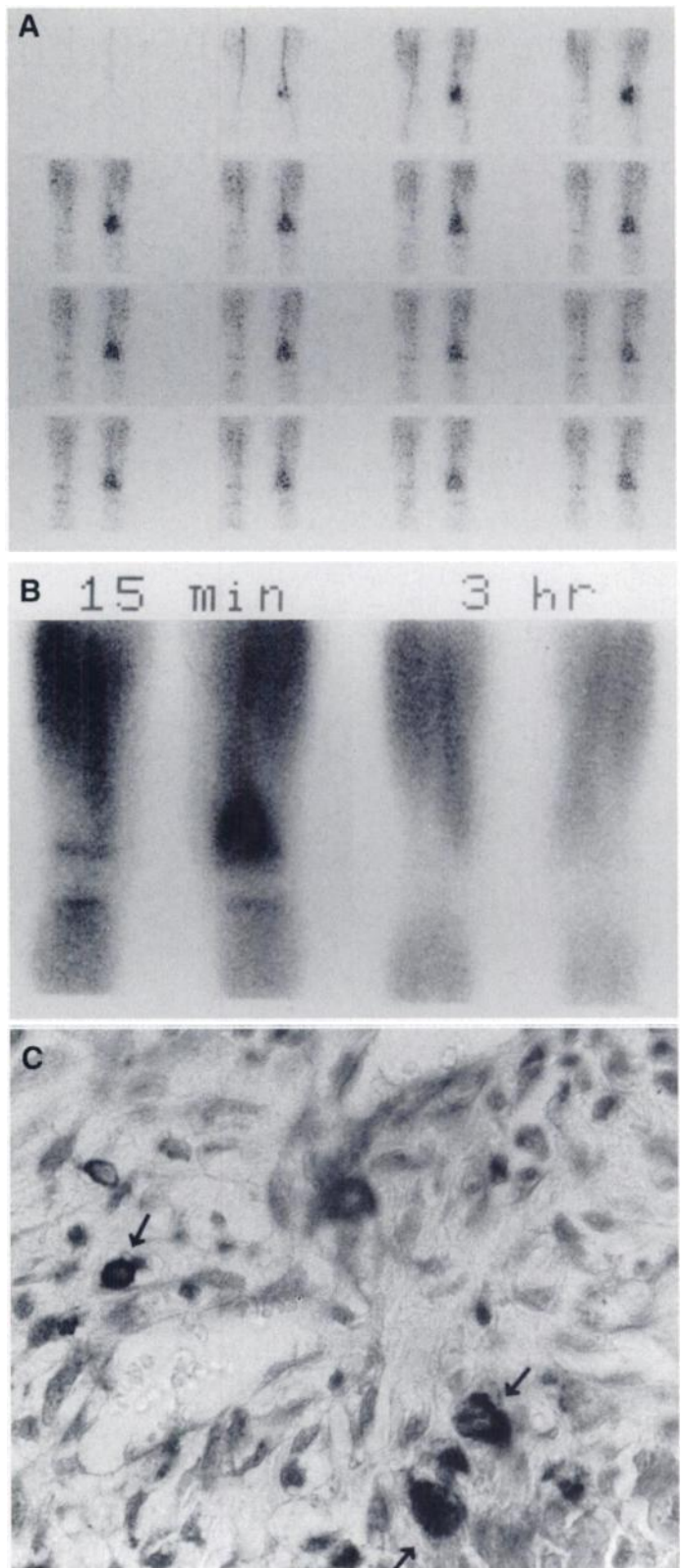


**FIGURE 2.** A 9-yr-old girl with osteosarcoma of left distal femur (Patient 28). (A) Radionuclide angiography with  $^{99m}\text{Tc}$ -MIBI demonstrated hypervascular lesion. (B) Technetium-99m-MIBI scintigraphy showed intense tracer uptake in 15-min image; 3-hr image showed complete  $^{99m}\text{Tc}$ -MIBI washout. (C) Immunohistochemical staining for P-glycoprotein showed positive reactions in Golgi area of more than 50% of osteosarcoma cells (Score 3) (arrows). Nuclear stain with hematoxylin,  $\times 300$ .

were stained; (c) Score 2 when 10% to 49% of the cells were stained; and (d) Score 3 when 50% or more of the cells were stained.

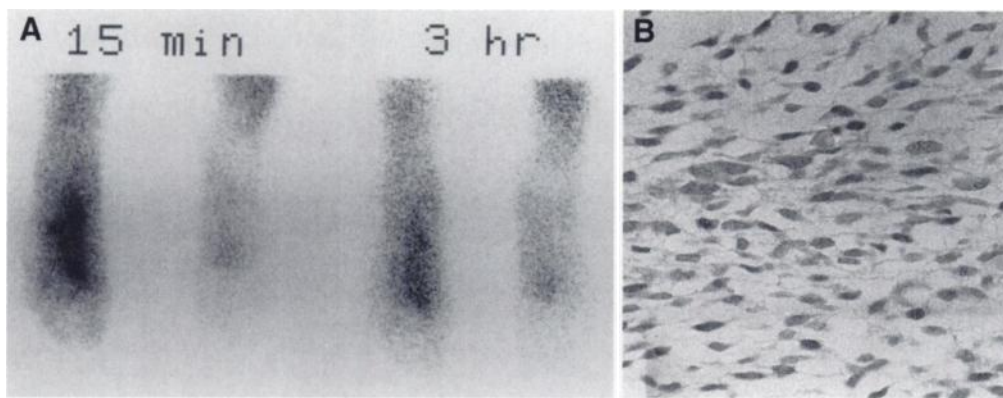


**FIGURE 3.** A 35-yr-old woman with synovial cell sarcoma in left plantar (Patient 7). (A) High  $^{99m}\text{Tc}$ -MIBI uptake was observed in 15-min image with minimal  $^{99m}\text{Tc}$ -MIBI washout in 3-hr image. (B) Immunohistochemical staining showed no significant Pgp expression (Score 0). Nuclear stain with hematoxylin,  $\times 300$ .

### Statistics

Values are presented as mean  $\pm$  s.d. Univariate analyses were performed using a two-tailed unpaired Student's t-test. The correlation between Pgp expression level and the washout rate of  $^{99m}\text{Tc}$ -MIBI was determined using the Spearman's rank correlation coefficient. The pairwise comparisons of these with the  $^{99m}\text{Tc}$ -MIBI washout rate in different Pgp levels were performed using Bonferroni's (Dunn's) test as a posthoc analysis after detecting significance with the Kruskal-Wallis test. Comparison of proportion was performed with a chi-square test and  $p < 0.05$  was considered significant. To account for multiple testing, a Bonferroni correction of the nominal probability value was performed, when appropriate.

### RESULTS

All patients' data were tabulated in Table 1. In the visual analysis, 24 of 30 patients showed significant uptake at the 15-min image. In these 24 patients, the Pgp score was 0 in 4 patients, 1 in 5 patients, 2 in 9 patients and 3 in 6 patients. Technetium-99m-MIBI accumulation disappeared at the 3-hr imaging in 7 patients (complete washout). When the high Pgp expression was defined as a score of 2 or more, patients with a high Pgp expression showed a more complete washout of  $^{99m}\text{Tc}$ -MIBI than the patients without a high Pgp expression (7 of 15 patients versus 0 of 9 patients,  $p < 0.05$ ). In 6 patients without  $^{99m}\text{Tc}$ -MIBI uptake at the 15-min image, the score of the Pgp expression was 0 in 4 patients and 2 in 2 patients. None of these patients without  $^{99m}\text{Tc}$ -MIBI uptake at the 15-min imaging showed  $^{201}\text{Tl}$  uptake.

In quantitative analysis in patients with a visual uptake score of 1 or more in early images, patients with a high Pgp expression showed a similar  $^{99m}\text{Tc}$ -MIBI perfusion index ( $3.00 \pm 1.04$ ) and uptake ratio ( $2.05 \pm 0.58$ ) at the early image compared to those of patients without a high Pgp expression ( $2.65 \pm 0.85$ ,  $p = 0.38$  and  $2.28 \pm 0.64$ ,  $p = 0.40$ , respectively). On delayed images, the  $^{99m}\text{Tc}$ -MIBI uptake ratio was lower in patients with a high Pgp expression than in patients without a high Pgp expression ( $1.37 \pm 0.41$  versus  $1.87 \pm 0.39$ ,  $p < 0.01$ ). The washout rate of  $^{99m}\text{Tc}$ -MIBI was higher in patients with a high Pgp expression than in those without a high Pgp expression ( $66\% \pm 25\%$  versus  $29 \pm 18$ ,  $p < 0.001$ ). The relationship between the Pgp score and the  $^{99m}\text{Tc}$ -MIBI washout rate is shown in Figure 1. The washout rates of  $^{99m}\text{Tc}$ -MIBI in patients with Pgp scores of 0, 1, 2, 3 were  $27\% \pm 21\%$ ,  $30\% \pm 18\%$ ,  $59\% \pm 22\%$ ,  $75\% \pm 27\%$ , respectively. Positive correlation between the Pgp score and the washout rate of  $^{99m}\text{Tc}$ -MIBI was observed ( $r = 0.642$ ,  $p < 0.005$ ). Significant differences in the  $^{99m}\text{Tc}$ -MIBI washout were observed between patients with Pgp scores of 0 and 3 ( $p < 0.005$ ) and between patients with scores of 1 and 3 ( $p < 0.005$ ).

Representative patients are shown in Figures 2, 3 and 4.

Figure 2 shows a 9-yr-old girl with osteosarcoma of the left distal femur (Patient 28). Radionuclide angiography revealed a hypervascular lesion. Technetium-99m-MIBI demonstrated intense tracer uptake in the 15-min image; however, the 3-hr image showed no significant tracer uptake. Immunohistochemical staining of the biopsy specimen showed a high Pgp expression (Score 3).

Figure 3 shows a 35-yr-old woman with synovial cell sarcoma in the left planta pedis (Patient 7). High  $^{99m}\text{Tc}$ -MIBI uptake was observed in the 15-min image with minimal  $^{99m}\text{Tc}$ -MIBI washout at the 3-hr image. No significant Pgp expression was observed.

Figure 4 shows a 48-yr-old man with fibromyxoid sarcoma in the left calf with bone invasion (Patient 29). Radionuclide angiography showed a hypervascular lesion. High  $^{99m}\text{Tc}$ -MIBI accumulation was observed in the lesion in the 15-min image. The 3-hr image showed complete  $^{99m}\text{Tc}$ -MIBI washout from the lesion. Immunohistochemical staining revealed a high Pgp expression (Score 3).

### DISCUSSION

Our data revealed that increased  $^{99m}\text{Tc}$ -MIBI washout indicated Pgp overexpression in malignant bone and soft-tissue tumors, while the perfusion index and early uptake ratio of  $^{99m}\text{Tc}$ -MIBI did not. For the evaluation of Pgp expression using  $^{99m}\text{Tc}$ -MIBI in patients with malignant bone and soft-tissue tumors, the combination of early and delayed imaging should be performed and washout analysis is recommended.

Several in vitro studies have shown that the  $^{99m}\text{Tc}$ -MIBI uptake by tumor cells is suppressed by increased expression of plasma cell membrane Pgp, which has been detected in all forms of human cancers (10,20). In vitro, once  $^{99m}\text{Tc}$ -MIBI had accumulated in cells with Pgp, it was effluxed rapidly from the cells and its efflux was inhibited by verapamil, a Pgp-reversing agent (13). In an in vivo study using rats, it was shown also that the washout of the  $^{99m}\text{Tc}$ -MIBI was three times faster in breast adenocarcinoma of the doxorubicin-resistant variant than its wild type, which had very low levels of Pgp (14). In humans, the biliary surface of hepatocytes and the proximal tubules of the kidneys normally have Pgp, and clearance of  $^{99m}\text{Tc}$ -MIBI from the liver and kidneys is inhibited significantly by the SDZ PSC 833, a second-generation modulator of MDR Pgp and a nonimmunosuppressive analog of cyclosporins A and D (21).

Several articles have focused on evaluating multidrug resistance using  $^{99m}\text{Tc}$ -MIBI in patients with malignant tumors including breast cancer, lymphoma, renal cell cancer and small-cell lung cancer, but none of them assessed  $^{99m}\text{Tc}$ -MIBI washout from the tumors (22–26). Most of these studies suggested that the absence of  $^{99m}\text{Tc}$ -MIBI uptake up to 30 min after injection was an indicator of Pgp expression. However, Del Vecchio et al. (22) showed high early uptake of  $^{99m}\text{Tc}$ -

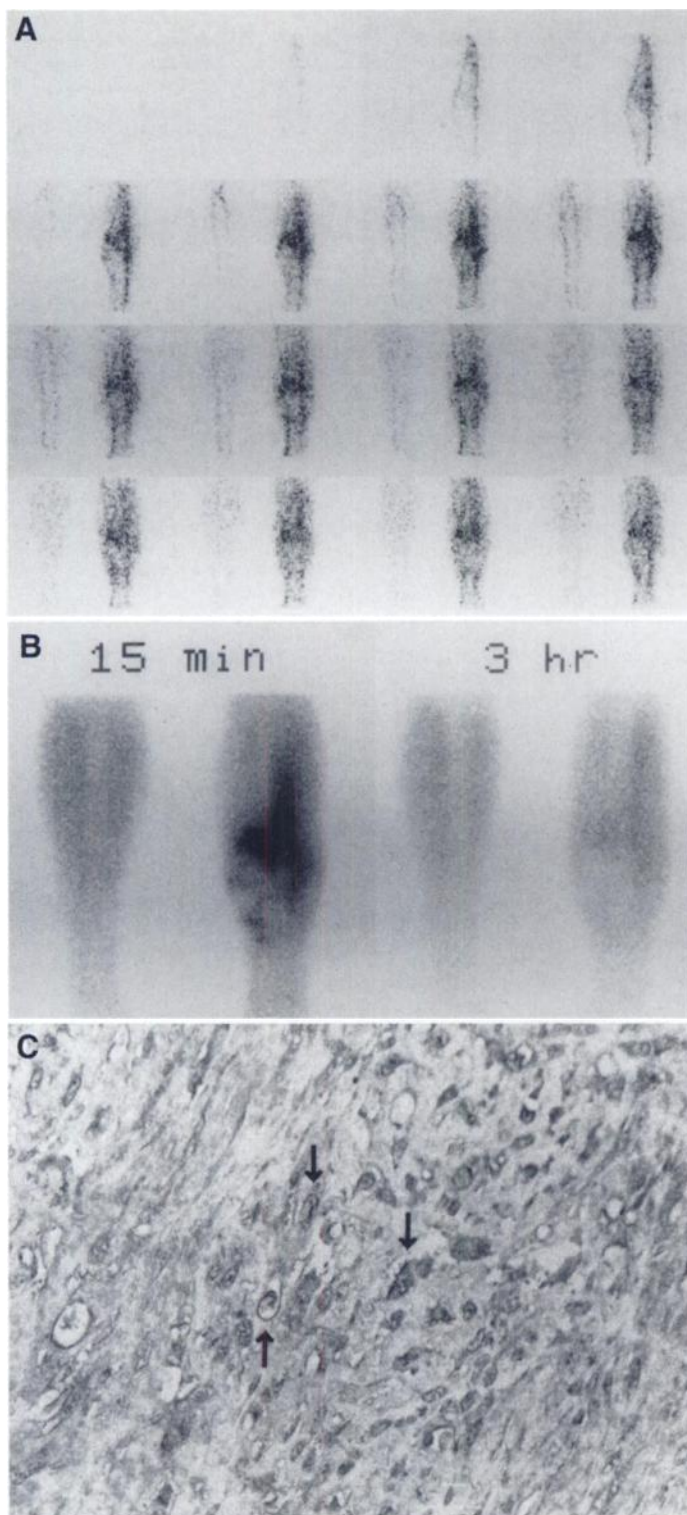


**FIGURE 4.** A 48-yr-old man with fibromyxoid sarcoma in left calf (Patient 29). (A) Radionuclide angiography showed a hypervascular lesion. (B) High  $^{99m}\text{Tc}$ -MIBI uptake was observed in the lesion in 15-min image. Complete  $^{99m}\text{Tc}$ -MIBI washout from lesion was observed in 3-hr image. (C) Immunohistochemical staining revealed positive reaction on cell membrane of more than 50% tumor cells (Score 3) (arrows). Nuclear stain with hematoxylin,  $\times 300$ .

MIBI in breast cancer even in the tumors with a high Pgp expression, and  $^{99m}\text{Tc}$ -MIBI efflux from tumors with a high Pgp expression was 2.7 times faster than that observed in tumors without a high Pgp expression. This study also revealed that a significant uptake of  $^{99m}\text{Tc}$ -MIBI at 15 min postinjection was observed in malignant bone and soft-tissue tumors, both with and without high Pgp expression, and there was a positive

correlation between the  $^{99m}\text{Tc}$ -MIBI washout and the degree of Pgp expression. The tumors with absent  $^{99m}\text{Tc}$ -MIBI uptake were not related to a high Pgp expression (only 2 of 6 patients without  $^{99m}\text{Tc}$ -MIBI uptake showed a high Pgp expression) but were associated with the absent uptake of  $^{201}\text{Tl}$ , which is not a substrate for Pgp but a marker of perfusion and a viable cell component. Thus,  $^{201}\text{Tl}$  scintigraphy is recommended when  $^{99m}\text{Tc}$ -MIBI imaging shows absent uptake to verify whether absent  $^{99m}\text{Tc}$ -MIBI uptake is due to poor blood flow and/or poor cell component. Another approach for interpreting the absence of  $^{99m}\text{Tc}$ -MIBI uptake may be to perform radionuclide  $^{99m}\text{Tc}$ -MIBI angiography for evaluating perfusion since only 1 of 6 patients without  $^{99m}\text{Tc}$ -MIBI uptake showed increased perfusion. When significant uptake of the tracer is observed in the early image, delayed imaging should be performed to evaluate Pgp expression based on the degree of the  $^{99m}\text{Tc}$ -MIBI washout.

Clinically, overexpression of Pgp correlated with a poor chemotherapeutic response and poor prognosis in many instances including bone and soft-tissue tumors (17,27–30). Therefore, recognition of Pgp is considered useful in patient management. In malignant bone and soft-tissue tumors, doxorubicin, a transport substrate for Pgp, is generally effective and is included in chemotherapy protocols (31). Recognition of the overexpression of Pgp before initiation of chemotherapy may be important and beneficial in patient management. If modulation of Pgp becomes feasible in clinical practice,  $^{99m}\text{Tc}$ -MIBI scintigraphy would be useful as a Pgp function monitoring method.

Several methods have been used to evaluate Pgp expression in human tissues. The majority of studies have used bulk techniques (Northan, Western or dot blotting) for detecting and quantifying Pgp and its mRNA. In these methods, however, Pgp in a large variety of normal tissues and cells cannot be distinguished from Pgp expressed in tumor cells (16). Accordingly, the immunohistochemical detection system appears more practical, hence, we performed immunohistochemical analysis semiquantitatively for detecting Pgp. We evaluated the degree of Pgp expression based on the distribution of immunostaining positivity, but not on the degree of staining, because the degree of staining is more objective than the distribution of positivity. The quantitative method for measuring Pgp expression with immunohistochemical staining with an autoradiographic technique is preferable, although good correlation between semiquantitative grading with immunoperoxidase staining and quantitative autoradiography was demonstrated (22).

Although MDR1 mRNA levels were relatively consistent in different portions of the osteosarcomas (32), Pgp distribution might be heterogeneous in other tumors, in which case the Pgp score determined by the small biopsy specimen might not always indicate whole-tumor Pgp expression, obscuring the correlation of the Pgp score and the  $^{99m}\text{Tc}$ -MIBI washout. In the current study, a biopsy was performed to obtain a specimen from the front of the tumor invasion where the Pgp expression was usually high. It was about fingertip size and was the only small part of the tumors. We could not examine the precise heterogeneity of Pgp expression throughout the tumor. Technetium-99m-MIBI scintigraphy, on the contrary, shows whole-tumor uptake and washout. In our study, we did not observe any patient with heterogeneous  $^{99m}\text{Tc}$ -MIBI washout from the lesion. Spatial resolution of planar scintigraphy might be insufficient to delineate the inhomogeneous washout of  $^{99m}\text{Tc}$ -MIBI if the heterogeneity of Pgp expression is present. Technetium-99m-MIBI can accumulate to peritumoral stromal tissue and modify regional uptake and washout kinetics. Poor perfu-

sion and cellular content, on the other hand, can be related to poor  $^{99m}\text{Tc}$ -MIBI uptake. Another factor influencing the correlation between Pgp expression and  $^{99m}\text{Tc}$ -MIBI washout may be the possibility of the uncoupling of Pgp expression and function. In acute myeloid leukemia cell lines, immature cell lines with lower expressions of Pgp showed transport activity, while mature cells with a high expression of Pgp did not transport Pgp substrates (33). However,  $^{99m}\text{Tc}$ -MIBI scintigraphy might permit in vivo functional assay of Pgp activity more accurately than other methods, such as immunohistochemical detection of Pgp or measurement of MDR1 RNA levels.

We performed imaging at 15 min and 3 hr postinjection of the radiopharmaceutical, but only because 3-hr delayed imaging was convenient for a routine study. The timing of scintigraphy after injection of  $^{99m}\text{Tc}$ -MIBI, especially in delayed imaging, remains to be validated.

## CONCLUSION

In bone and soft-tissue tumors, perfusion and initial  $^{99m}\text{Tc}$ -MIBI uptake were not related to the Pgp expression; however, washout of  $^{99m}\text{Tc}$ -MIBI from the tumor was related to Pgp expression. High washout of  $^{99m}\text{Tc}$ -MIBI indicated overexpression of Pgp. Technetium-99m-MIBI scintigraphy with washout analysis may be a useful method for evaluating Pgp overexpression and its function.

## ACKNOWLEDGMENTS

This study was partly supported by a Grant for Project Research from Kanazawa Medical University (P95-14 and P96-2).

## REFERENCES

- Aktolun C, Bayhan H and Kir M. Clinical experience with  $^{99m}\text{Tc}$ -MIBI imaging in patients with malignant tumors. Preliminary results and comparison with Tl-201. *Clin Nucl Med* 1992;17:171-176.
- O'Tuama LA, Treves ST, Larar JN, et al. Thallium-201 versus technetium-99m-MIBI SPECT in evaluation of childhood brain tumors: a within-subject comparison. *J Nucl Med* 1993;34:1045-1051.
- Balon HR, Fink BD and Stoffer SS. Technetium-99m-sestamibi uptake by recurrent Hürthle cell carcinoma of the thyroid. *J Nucl Med* 1992;33:1393-1395.
- Scott AM, Kostakoglu L, O'Brien JP, et al. Comparison of technetium-99m-MIBI and thallium-201-chloride uptake in primary thyroid lymphoma. *J Nucl Med* 1992;33:1396-1398.
- Desai SP and Yuille DL. Visualization of a recurrent carcinoid tumor and an occult distant metastasis by technetium-99m-sestamibi. *J Nucl Med* 1993;34:1748-1751.
- Caner B, Kitapci M, Unlu M, et al. Technetium-99m-MIBI uptake in benign and malignant bone lesions: a comparative study with technetium-99m-MDP. *J Nucl Med* 1992;33:319-324.
- Taki J, Sumiya H, Tsuchiya H, Tomita K, Nonomura A, Tonami N. Evaluating benign and malignant bone and soft tissue lesions with technetium-99m-MIBI scintigraphy. *J Nucl Med* 1997;38:501-506.
- Link MP, Goorin AM, Horowitz M, et al. Adjuvant chemotherapy of high-grade osteosarcoma of the extremity: updated results of the multi-institutional osteosarcoma study. *Clin Orthop* 1991;270:8-14.
- Rosen G. Neoadjuvant chemotherapy for osteogenic sarcoma: a model for the treatment of other highly malignant neoplasms. *Recent Results Cancer Res* 1986;103:148-157.
- Rao VV, Chiu ML, Kronauge JF, Piwnica-Worms D. Expression of recombinant human multidrug resistance p-glycoprotein in insect cells confers decreased accumulation of technetium-99m-sestamibi. *J Nucl Med* 1994;35:510-515.

- Endicott JA, Ling V. The biochemistry of P-glycoprotein-mediated multidrug resistance. *Annu Rev Biochem* 1989;58:137-171.
- Noonan KE, Beck C, Holzmayer TA, et al. Quantitative analysis of MDR1 (multidrug resistance) gene expression in human tumors by polymerase chain reaction. *Proc Natl Acad Sci USA* 1990;87:7160-7164.
- Piwnica-Worms D, Chiu ML, Budding M, Kronauge JF, Kramer RA, Croop JM. Functional imaging of multidrug-resistant P-Glycoprotein with an organotechnetium complex. *Cancer Res* 1993;53:997-984.
- Ballinger JR, Hua HA, Berry BW, Firby P, Boxen I. 99Tcm-sestamibi as an agent for imaging P-glycoprotein-mediated multi-drug resistance: In vitro and in vivo studies in a rat breast tumor cell line and its doxorubicin-resistant variant. *Nucl Med Commun* 1995;16:253-257.
- Cordobes MD, Starzec A, Delmon-Moingeon L, et al. Technetium-99m-sestamibi uptake by human benign and malignant breast tumor cells: correlation with MDR gene expression. *J Nucl Med* 1996;37:286-289.
- Roessner A, Ueda Y, Bockhorn-Dwomiczak B, et al. Prognostic implication of immunodetection of P glycoprotein in Ewing's sarcoma. *J Cancer Res Clin Oncol* 1993;119:185-189.
- Baldini N, Scotlandi K, Barbanti-Brodano G, et al. Expression of P-glycoprotein in high-grade osteosarcomas in relation to clinical outcome. *N Engl J Med* 1995;333:1380-1385.
- Van der Valk P, Van Kalken CK, Ketelaars H, et al. Distribution of multidrug resistance-associated P-glycoprotein in normal and neoplastic human tissues: analysis with 3 monoclonal antibodies recognizing different epitopes of the P-glycoprotein molecule. *Ann Oncol* 1990;1:56-64.
- O'Meara A, Imamura A, Johnson P, et al. Reactivity of P-glycoprotein monoclonal antibodies in childhood cancers. *Oncology* 1992;49:203-8.
- Goldstein LJ, Galski H, Fojo A, et al. Expression of a multidrug resistance gene in human cancers. *J Natl Cancer Inst* 1989;81:116-124.
- Luker GD, Fracasso PM, Dobkin J, Piwnica-Worms D. Modulation of the multidrug resistance P-glycoprotein: detection with Technetium-99m-sestamibi in vivo. *J Nucl Med* 1997;38:369-372.
- Del Vecchio S, Ciarniello A, Potena MI, et al. In vivo detection of multidrug-resistant (MDR1) phenotype by technetium-99m sestamibi scan in untreated breast cancer patients. *Eur J Nucl Med* 1997;24:150-159.
- Derebeck E, Kirkali Z, Dogan S, et al. Technetium-99m-MIBI scintigraphy in metastatic renal cell carcinoma: clinical validation of the relationship between  $^{99m}\text{Tc}$ -MIBI uptake and P-glycoprotein expression in tumor tissue. *Eur J Nucl Med* 1996;23:976-979.
- Moretti JL, Caglar M, Boaziz C, Caillat-Vigneron N, Morere JF. Sequential functional imaging with technetium-99m hexakis-2-methoxyisobutylisonitrile and indium-111 octreotide: can we predict the response to chemotherapy in small cell lung cancer? *Eur J Nucl Med* 1995;22:177-180.
- Dimitrakopoulou-Strauss A, Strauss LG, Goldschmidt H, Lorenz WJ, Maier-Borst W, van Kaik G. Evaluation of tumor metabolism and multidrug resistance in patients with treated malignant lymphomas. *Eur J Nucl Med* 1995;22:434-442.
- Moretti JL, Azaloux H, Boisseron D, Kouyoumdjian JC, Vilcoq J. Primary breast cancer imaging with technetium-99m sestamibi and its relation with P-glycoprotein overexpression. *Eur J Nucl Med* 1996;23:980-986.
- Serra M, Scotlandi K, Manara MC, et al. Analysis of P-glycoprotein expression in osteosarcoma. *Eur J Cancer* 1995;31A:1998-2002.
- Chan HSL, Thorne PS, Haddad G, Ling V. Immunohistochemical detection of P-glycoprotein: prognostic correlation in soft tissue sarcoma of childhood. *J Clin Oncol* 1990;8:689-704.
- Chan HSL, Haddad G, Thorne PS, et al. P-glycoprotein expression as a predictor of the outcome of therapy for neuroblastoma. *N Engl J Med* 1991;325:1608-1614.
- Norris MD, Bordow SB, Marshall GM, Haber PS, Cohn SL, Haber M. Expression of the gene for multidrug-resistance-associated protein and outcome in patients with neuroblastoma. *N Engl J Med* 1996;334:231-238.
- Priebat DA, Trehan RS, Malawer MM, Chulof RS. Induction chemotherapy for sarcoma of the extremities. In: Sugarbaker PH, Malawer MM, eds. Musculoskeletal surgery for cancer: principle and techniques. New York: Thieme Medical Publishers; 1992:96-120.
- Lee PD, Noble-Topham SE, Bell RS, Andrusis IL. Quantitative analysis of multidrug resistance gene expression in human osteosarcomas. *Br J Cancer* 1996;74:1046-1050.
- Bailey JD, Muller C, Jaffrezou JP, et al. Lack of correlation between expression and function of P-glycoprotein in acute myeloid leukemia cell lines. *Leukemia* 1995;9:799-807.